Electron Vacuum Acceleration in a Regime beyond Brunel Absorption

J. P. Geindre,[1] R. S. Marjoribanks,[2,*] and P. Audebert[1]

[1]*Laboratoire pour l'Utilisation des Lasers Intenses (LULI), Ecole Polytechnique Route de Saclay, 91128 Palaiseau cedex, France*

[2]*Department of Physics, & Institute for Optical Sciences University of Toronto, 60 St. George Street, Toronto, Ontario, M5S 1A7, Canada*

(Received 1 May 2009; published 30 March 2010)

We describe a new regime of electron acceleration in laser plasmas driven by ultrafast pulses of relativistic intensity, in which space-charge separation leads to strongly enhanced laser absorption and the production of 20 MeV ($p/m_0c \approx 40$) electrons driven outward in vacuum. 1D PIC simulations show that intense attosecond pulses generated around critical density can sweep electrons outward over many wavelengths in distance. With increasing interaction scale length, absorption generalizes from the Brunel regime to one in which absorption is primarily into electrons of energy $\gg 5$ MeV.

DOI: 10.1103/PhysRevLett.104.135001 PACS numbers: 52.38.Kd, 42.65.Ky, 52.38.Fz

Introduction.—Mechanisms of light absorption in laser-produced plasmas are probably the most central and constant issue in the field, since their details determine much of the particle dynamics and energy partitioning in a laser plasma. In the most general terms, the issue is how laser-driven oscillatory power is coupled to electron collective motion, dissipated to thermal motion, and from there shared out to secular motion of ions, via the ambipolar field set up by space-charge separation.

In nanosecond laser plasmas, the large number of well-established mechanisms of absorption include inverse-Bremsstrahlung, stimulated Raman, and stimulated Brillouin absorption, in the underdense plasma, and resonance absorption in the gradient around critical density. The electron-density scale length around critical density is perhaps the most significant single parameter, for it is near the critical surface that resonance absorption and wave breaking of driven waves leads to electron acceleration, thermal dissipation, and heating. In this process, ponderomotive steepening self-consistently determines the absorption, and scale lengths $[d(\log N_e)/dx]^{-1} = 0.1\lambda$ can typically be produced, at high values of the kinetic parameter $I\lambda^2$ [1].

For laser plasmas produced using high-contrast femtosecond pulses, sharp-boundary plasmas are the natural result of short time scales. For such ultrafast pulses at high intensities, and at non-normal incidence, "vacuum absorption," first described by Brunel [2], becomes a very important mechanism: in gradients too steep for resonant absorption, electrons driven by the laser near the critical-density surface can be separated from the bulk of the oscillating plasma, acquire kinetic energy as they execute phase-shifted half-cycle orbits, and subsequently deposit their accumulated energy behind the critical surface.

In the last decade, numerical simulations by many researchers have been seminal: revealing the physics of ultrafast absorption on solid targets, and of electron and ion acceleration under laser irradiances that force relativistic motion. Different conditions of the plasma profile have proved to be important, among them: different electron-density gradients at the critical surface; different overdense shelf densities behind the critical surface; and different size scales for focal spots, from uniform 1D geometry to large-divergence wavelength-scale focal spots [3]. Changing these conditions can steer the interaction outcome: for instance, the formation of strong quasistatic plasma fields, which can in turn accelerate particles, from the front and from the rear surfaces of targets [4].

Such control of the interaction becomes more subtle at relativistic intensities, when electrons oscillating near the speed of light see strong plasma E fields as strong time-dependent B fields. For the EM field, the ratio $E/B = 1$ *in vacuo* is unique in context of the Lorentz transformation: we have recently described how departure from that ratio (e.g., because of partial cancellation of E in p-polarized light in oblique reflection at a plasma mirror surface) will lead to unexpected latent fields which inhibit and tangle the trajectories of the electrons, and frustrate efforts to make a more relativistic plasma by intensity increases alone [5]. Conversely, in vacuum, acceleration of free electrons to MeV energies by relativistically intense optical fields has been demonstrated experimentally [6].

In this Letter we describe a new regime of absorption, in which plasma space-charge separation and resultant increased E fields around critical change the nature of half-cycle Brunel absorption, leading to direct vacuum acceleration of electrons by the *outgoing* attosecond optical field, over propagation distances of many wavelengths.

Emergence of space-charge effects.—The systematic effects of plasma fields can be illustrated by numerical modelling of ultraintense interaction with plasmas of different fixed scale lengths. Figure 1 shows one-dimensional particle-in-cell (1D PIC) simulations using the code EUTERPE [7]. In all cases $I = 4 \times 10^{19}$ W/cm^2 ($a_0 \approx 5$) and $\lambda = 1$ μm; the pulse envelope has a $\sin^2(t)$ form with FWHM 12 fs. All simulations use immobile ions for simplicity, to isolate effects of scale length; for our few-cycle pulses, mobile-ion calculations show no significant differ-

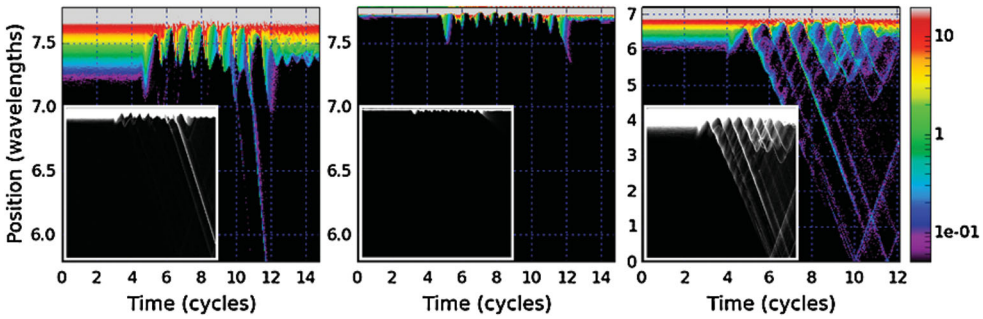

FIG. 1 (color). 1D PIC modeling of 12-fs (FWHM) optical pulses of intensity $I = 4 \times 10^{19}$ W/cm^2, $\lambda = 1$ μm ($a_0 \approx 5$), incident at 45° on $N_e = 80N_c$ plasma, with fixed ions. Different transition scale lengths L: (a) $L = 0.076\lambda$, (b) $L = 0$, (c) $L = 0.15\lambda$. Inset figures repeat the data with single shared spatial scale, for global comparison [color scale: $\log_{10}(N_e/N_c)$].

ence. Prescribed density gradients are initially quasineutral, exponential with an upper-shelf electron density of $80N_c$. The angle of incidence is 45°, modeled in 1D using the well-known relativistic boosted-frame-of-reference approach.

Brunel-like absorption.—Figure 1(a) shows results from a gradient of scale length $L = [d(\log N_e)/dx]^{-1} = 0.076\lambda$. In this typical case, absorption is mainly by the mechanism of Brunel "vacuum absorption": field extraction of electrons, acceleration over a half cycle of laser, and injection of these hot electrons into the overdense region, vanishing behind critical density. This is considered the principal mechanism of absorption for ultrafast pulses incident on sharp gradients; absorption efficiency in this example is 22%, the electron distribution shows a sharp cutoff at $E_{\max} = 3.5$ MeV ($p/m_0c \approx 6.8$), and few electrons above this. Multiple attosecond pulses are generated by the surface oscillation: their peak power is observed to be 1.8× the incident laser power, in a single 200 attosecond pulse each incident laser cycle.

Brunel absorption frustrated by latent fields.—Figure 1(b) shows the same conditions as Fig. 1(a), but with incidence on a perfect density step (i.e., $L = 0$). Absorption efficiency in this case is merely 3%; the electron distribution has a sharp cutoff at $E_{\max} = 2.2$ MeV ($p/m_0c \approx 4.2$). In this sharp gradient, the superposition of incident and reflected p-polarized light gives a reduced electric field, compared to the B field: they no longer have the balance of an *EM* field in vacuum. At relativistic intensities, this results in gyromagnetic motion which inhibits laser-driven oscillation; higher laser intensities do not translate to more-relativistic laser plasmas. For this perfectly sharp gradient, there may be multiple attosecond pulses each laser cycle, following the complex motion of the magnetically constrained interface; the peak power of the attosecond optical pulses produced is seen to be reduced to merely 5% of the incident laser peak power.

What physical changes are responsible for the difference between this "frustrated" case and the "Brunel" case? The change in scale length of the initial density gradient, between the two cases, means greater penetration of the laser field in the Brunel case. Within this small gradient, the ponderomotive force drives a separation of charge, pushing electrons through the ion background, and creates a quasistatic E field directed inward. During a half cycle, this field adds with the E field of the laser: the gyromagnetic inhibition largely vanishes, and energy may be systematically transferred from laser to electrons—standard half-orbit Brunel absorption. These changes in E fields, for different-gradient scale lengths, are the essential difference that permit much greater absorption.

Absorption enhanced by space-charge fields.—As the prescribed initial gradient scale length is increased further, electrons are pushed inward during almost a half cycle, through an increasing distance, before being accelerated outward during the second part of the cycle, by the net electrostatic and *EM* E field. We note that this acceleration takes place inside the ion gradient. This push-pull mechanism leads to faster electron acceleration up to energies around 9 MeV ($p/m_0c \approx 18$) at $L = 0.1\lambda$.

Note that under this condition, assumptions used under Brunel-type modeling are no longer valid, as electron velocities approach c, and oscillation amplitudes are not small compared to the *EM* wavelength. Moreover, as the reflected *EM* field acquires high-harmonic content due to relativistic electron motion, it no longer has the form of the incident field—the *net EM* field is no longer a standing wave. Thereafter, propagation of the reflected field must be taken into account, as electron velocities become comparable to the *EM* phase velocity. Qualitatively new behavior can be expected in this new regime.

Attosecond-bunch vacuum acceleration (ABVA).—At longer-gradient scale lengths, indeed new behavior appears in our simulation modeling. Figure 1(c) shows the results of the same incident laser field as parts (a) and (b), but with an electron-density scale length $L = 0.15\lambda$. The results are quite different. Absorption efficiency in this case is 32%, and the electron distribution has its cutoff at a much higher $E_{\max} = 20$ MeV ($p/m_0c \approx 40$)—more than 5 times the typical "Brunel" case above. The reasons for this are apparent: instead of acquiring energy in well-phased half cycles of the laser, and depositing their energy behind critical, large numbers of electrons are now accelerated *secularly*, in the outgoing *EM* field, over distances of many

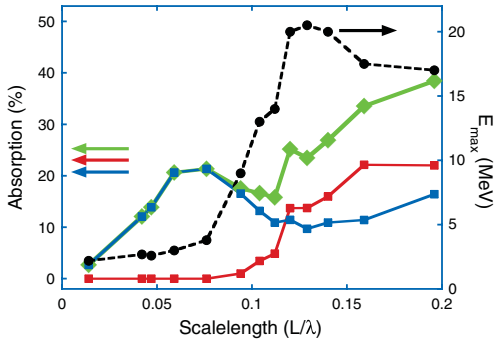

FIG. 2 (color). Absorption of 12 fs pulses ($I = 4 \times 10^{19}$ W/cm^2, $\lambda = 1$ μm) vs preformed plasma scale length L, shows a transition from typical Brunel absorption ($L < 0.1\lambda$) to much-enhanced net absorption and peak electron energy ($L > 0.1\lambda$). Blue curve: into electrons of energies <5 MeV; red curve: into electrons of energies >5 MeV; green curve: total absorption; black curve: peak electron energy produced.

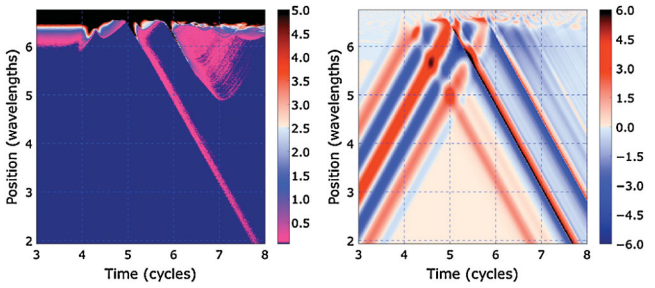

FIG. 3 (color). Same as Fig. 1, but 4 fs pulse, 1 cycle FWHM. (a) electron density N_e [color scale: $\log_{10}(N_e/N_c)$]; (b) electric-field amplitude E. Positive electric fields (red) point toward the target, accelerating electrons outward from the target. A single electron bunch is entrained with the outgoing attosecond pulse, and accelerated secularly during many laser periods.

laser wavelengths in the laboratory frame of reference. As this secular acceleration continues to bring electrons further from the target, they steadily slip out of the accelerated bunches, and are later driven back into the target by the space-charge field.

Absorption dependence on gradient scale length.—The picture of this distinct phenomenon of acceleration emerges more clearly when the net absorption at times late in the pulse is modeled as a function of the scale length of the preformed plasma. Figure 2 shows the total absorption fraction, and the breakdown of the absorbed energy according to electron energy.

The electron-energy cutoff for conditions of Fig. 1(a), typical of Brunel absorption, was 3.5 MeV. Figure 2 shows the breakdown of absorbed energy into such electrons (less than 5 MeV, blue curve), or more-energetic electrons (greater than 5 MeV, green curve). The figure makes it clear that with the rise of vacuum acceleration of electron bunches outward, with increasing scale length, it is not simply that increasingly energetic electrons are being added to the established distribution. Instead, absorption into electrons of energy <5 MeV decreases, the energy repartitioned to the cohort >5 MeV. The dynamics show a transition to a different vacuum-absorption mechanism, making two regimes of absorption.

Vacuum acceleration by attosecond fields.—To isolate the physical effects contributing to Fig. 1, Fig. 3 models a 4 fs (1 cycle) FWHM Gaussian pulse, generating a single attosecond reflected pulse. Figure 3(a) shows the electron density, particularly the dynamics of electron acceleration; Fig. 3(b) details the total accelerating field: the *EM* field of the incident laser, the *EM* field of the outgoing attosecond pulse, and the E field established by the space charge withdrawn from around critical density.

Naturally, the superposition of incoming and strongly reflected and modified *EM* fields near the critical-density surface is limited in extent, and structured, since the laser pulse is quite brief, and the attosecond reflected field is phase compressed, in the simple sense of the relativistic oscillating-mirror model [8]. Of particular interest, far from the critical-density surface, essentially in vacuum, a single electron bunch is observed to be superimposed on the trailing edge of the attosecond pulse.

The space charge of this escaped electron bunch plays a significant role also in the dynamics of electrons extracted on subsequent cycles. In the absence of accelerated electrons, the reflected *EM* field normally would have a second attosecond peak, but here it is effectively biased by the space-charge fields of electrons already extracted, and the fields in the region between the attosecond pulse and the critical surface are all negative—directed for accelerating electrons back to the target. Out of the electron bunch entrained with the outgoing attosecond pulse there is a steady leak of electrons into this region, whereupon they are rapidly sent back to the target. For a second bunch of electrons extracted from around critical density, there is no acceleration: we observe complete electrostatic reflection of the second extracted bunch back to the target, in our simulation, whenever the first bunch extracted comprises a sufficiently large charge.

Phase-space summary.—Figure 4 shows 7 snapshots in time of the (x-P_x) distribution of the single bunch of electrons during acceleration. Here the secular growth is clear: electrons continue to be accelerated, to increasingly high cutoff energies, but as electrons are accelerated and contribute to space charge well outside the critical-density surface, more and more electrons, carried to progressively higher potentials, slip back from the attosecond field and return to the target with progressively increasing energies.

Discussion.—The physical picture of this new regime of absorption and vacuum acceleration in relativistic ultrashort laser-plasma interaction comprises two distinct phases: qualitative changes in the relativistic relationship between driving fields, electron trajectories and space-charge fields, as they affect extraction of electrons near critical; and acceleration of electrons by attosecond pulses in vacuum, over many wavelengths in the lab frame.

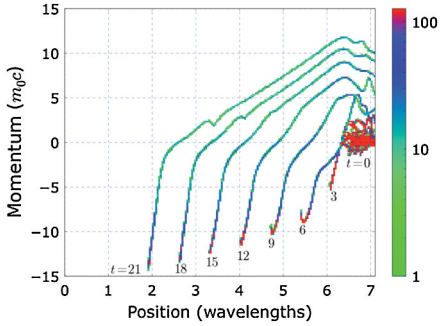

FIG. 4 (color). 7 snapshots in time (at intervals of three laser cycles) of the (x, P_x) phase-space distribution of electrons as in Fig. 3. One electron bunch is accelerated monotonically outward over the time of many laser cycles.

In the first phase—extraction and injection—the plasma dynamics and electron trajectories around critical density are strongly affected by the destructive interference of the laser E field on reflection, with relativistic implications as seen previously for the case of an abrupt-step perfect mirror [5]. Changes in this interference in a finite gradient, together with local changes in the space-charge fields, alter the simple perfect-mirror picture. These effects combine to produce electron trajectories with different phase relationships relative to the driving fields, and which differently inject electrons into the departing attosecond EM field.

In the second phase, the outward acceleration of electrons, in the strong field of the attosecond reflected pulses, raises questions about the transfer of energy between an EM field and free electrons in vacuum. For such pulses the intensity change is not even approximately adiabatic on the time scale of an optical period, and the carrier-envelope phase relationship is a significant factor in the transient field an electron will see. For the outgoing attosecond pulses generated here, the carrier-envelope phase relationship is determined by the incident laser carrier-envelope phase relationship and by the self-consistent plasma dynamics, and these together determine the harmonic spectrum and the form of the attosecond pulses. It is significant that the acceleration of outgoing electrons seen in these simulations is over many wavelengths in trajectory, and many laser cycles, both as measured in the laboratory frame. Note that in the relativistic frame of the escaped electron the vacuum-acceleration phase takes place during less than one cycle.

For a realistic laser focus, two-dimensional effects will likely come into play, degrading the reflected field intensities and limiting the longitudinal distance and time over which electrons are accelerated. At the same time, two-dimensional effects will probably mean that escape from the space-charge field will become easier, with the ultimate result of production of an energetic, intense and dense beam with very low emittance. Experimental observation of these effects may depend on using focal spot sizes of many wavelengths in diameter.

This leads naturally to several new questions. With the changes in absorption, and extraction of space charge, what will be the impact on ambipolar-field acceleration of fast ions? What will be the impact, on fields and net absorption, of longer pulses during which time fast ions may begin to be extracted and establish a density shelf around critical? How might this be modified for very much greater laser intensities?

Conclusions.—We have shown here, from one-dimensional PIC simulations using few-cycle pulses to set aside hydrodynamic evolution and with dictated initial density profiles, a regime of absorption and electron acceleration beyond classical Brunel absorption of relativistic ultrafast laser pulses in plasmas. Brunel-type absorption—with electrons executing canonical half-cycle trajectories while acquiring energy in a secular way from the laser field—is seen to be suppressed in the case of very steep electron-density gradients around critical, due to relativistic AC gyromagnetic effects accompanying suppression of the E field by destructive interference. At scale lengths longer than typical, there is a systematic shift: because of local fields developing from finite-gradient space charge, electrons may be differently phased with respect to the laser, extracted from the gradient, injected into very strong outgoing attosecond fields, and monotonically accelerated outward in vacuum to energies >20 MeV.

R. S. M. acknowledges the support of the Ecole Polytechnique (Directeur Général Adjoint Chargé de la Recherche), the Natural Sciences and Engineering Research Council of Canada (NSERC), and of the Canadian Institute for Photonic Innovations (CIPI).

*marj@physics.utoronto.ca

[1] R. Fedosejevs, I. V. Tomov, N. H. Burnett, G. D. Enright, and M. C. Richardson, Phys. Rev. Lett. **39**, 932 (1977).
[2] F. Brunel, Phys. Rev. Lett. **59**, 52 (1987).
[3] W. Yu *et al.*, Phys. Rev. Lett. **85**, 570 (2000); N. Naumova *et al.*, Phys. Rev. Lett. **93**, 195003 (2004).
[4] E. L. Clark *et al.*, Phys. Rev. Lett. **84**, 670 (2000); K. Krushelnick *et al.*, Phys. Plasmas **7**, 2055 (2000); A. Maksimchuk, S. Gu, K. Flippo, D. Umstadter, and V. Y. Bychenkov, Phys. Rev. Lett. **84**, 4108 (2000).
[5] J. P. Geindre, P. Audebert, and R. S. Marjoribanks, Phys. Rev. Lett. **97**, 085001 (2006).
[6] G. Malka, E. Lefebvre, and J. L. Miquel, Phys. Rev. Lett. **78**, 3314 (1997); E. Esarey, P. Sprangle, and J. Krall, Phys. Rev. E **52**, 5443 (1995).
[7] G. Bonnaud and C. Reisse, Nucl. Fusion **26**, 633 (1986).
[8] U. Teubner and P. Gibbon, Rev. Mod. Phys. **81**, 445 (2009).